Available online at www.sciencedirect.com
SCIENCE DIRECT®
Journal of Magnetic Resonance 166 (2004) 262–272
JMR Journal of Magnetic Resonance
www.elsevier.com/locate/jmr

A solid-state ^{14}N magic-angle spinning NMR study of some amino acids

Tania Giavani, Henrik Bildsøe, Jørgen Skibsted, and Hans J. Jakobsen*

Instrument Centre for Solid State NMR Spectroscopy, Department of Chemistry, University of Aarhus, DK-8000 Aarhus C, Denmark

Received 19 September 2003; revised 20 October 2003

Abstract

Experimental strategies for the acquisition of high-quality ^{14}N magic-angle spinning (MAS) NMR spectra of the simple amino acids, which exhibit ^{14}N quadrupole coupling constants (C_Q) on the order of 1.2 MHz, are devised. These are the first useful ^{14}N MAS spectra reported for nitrogen compounds having a $C_Q(^{14}N)$ value in excess of 1 MHz. The complete manifolds of spinning sidebands (ssbs), i.e., about 300 ssbs for a spinning frequency of 6.0 kHz, have been observed in the ^{14}N MAS NMR spectra of a series of amino acids. In their crystal structure these amino acids all exhibit the zwitterionic form and thus the ^{14}N MAS NMR spectra represent those of a rotating $-NH_3^+$ group and not of an amino ($-NH_2$) group. Computer simulations combined with fitting of simulated to the experimental ssb intensities result in the determination of precise values for the ^{14}N quadrupole coupling (C_Q) and its associated asymmetry parameter (η_Q) for the nitrogen sites in these molecules. For some of the amino acids the ^{14}N MAS NMR spectra exhibit overlap between the manifolds of ssbs from two different nitrogen sites in accordance with their crystal structures. Computer analysis of these spectra results in two different sets of (C_Q, η_Q) values which mainly differ in the magnitudes for η_Q.

1. Introduction

Along with hydrogen, carbon, and oxygen, the nitrogen atom constitutes the most important element in the chemistry of biomolecules and of many inorganic compounds related to materials sciences. Nuclear magnetic resonance (NMR) spectroscopies employing the ^{1}H, ^{13}C, ^{15}N, and ^{17}O spin isotopes of these atoms have been widely used in both liquid- and solid-state NMR studies of such materials. Most studies concerned with nitrogen NMR employ highly ^{15}N-enriched (and expensive) samples while the use of the natural abundant ^{14}N quadrupole spin isotope (99.7% abundance) has been quite limited. In particular this is true with respect to investigations related to the solid-state where only very few ^{14}N NMR studies have appeared. The reason is that traditionally the ^{14}N spin isotope in solids is considered very difficult to detect because of its low-γ properties, quite large quadrupole coupling constants (C_Q), and because its integer spin ($I = 1$) precludes the presence of the central transition as observed for half-integer quadrupolar nuclei. However, during the past few years solid-state ^{14}N magic-angle spinning (MAS) NMR spectroscopy has increased in quality, efficiency, and popularity [1–5], and with the most recent progress part of the experimental difficulties have been overcome. For example, complete ^{14}N MAS NMR spectra can now be successfully recorded for molecules (e.g., nitrate ions) characterized by ^{14}N quadrupolar couplings up to about 0.75 MHz [1–3].

The amino acids constitute an increase in the complexity of molecules which would be of interest to characterize by solid-state ^{14}N MAS NMR first of all because of their fundamental role in biochemistry as building blocks of peptides and proteins. Second, because of the 75–100% increase in C_Q as compared to the nitrates, ^{14}N MAS NMR of amino acids represents a challenge unresolved so far. During the 1970s many of the amino acids have been investigated by ^{14}N nuclear quadrupole resonance (NQR) spectroscopy [6–10], and several of their ^{14}N quadrupolar coupling parameters ($C_Q(^{14}N) \sim 1.2$ MHz) have been determined. With respect to solid-state NMR, a large number of studies on

* Corresponding author. Fax: +45-8619-6199.
E-mail address: hja@chem.au.dk (H.J. Jakobsen).

1090-7807/$ - see front matter © 2003 Elsevier Inc. All rights reserved.
doi:10.1016/j.jmr.2003.10.023

amino acids have been performed employing ^{13}C and ^{15}N as probes, while only few reports have appeared on applications employing ^{14}N NMR. The reason is that ^{14}N NMR is complicated by the need of particularly wide spectral widths, caused by large C_Q values (1–3 MHz), which spread the spectrum over a range up to 2 MHz or more. For such C_Q values a ^{14}N MAS NMR spectrum would display a very large number of spinning sidebands (ssbs), ranging from about 200 to 900 for a spinning speed of 5 kHz. While the complete ^{14}N MAS NMR spectrum for a polycrystalline powder of an amino acid has still to be presented, a few amino acids have been studied by ^{14}N single-crystal (SC) NMR, e.g., glycine [11,12], L-histidine hydrochloride monohydrate [13], L-asparagine monohydrate [14], and L-serine monohydrate [15]. We note that SC NMR is particularly useful for studies of samples characterized by large C_Q values, since the technique is capable of mapping the full width of a broad spectrum by detecting only a few quite narrow lines for each crystal orientation. Recently ^{14}N MAS NMR has gained renewed interest for the study of the most common amino acids. First, Jeschke and Jansen [16] claimed the detection of a ^{14}N MAS NMR ssb pattern for a sample of glycine. Following this report, Khitrin and Fung [5] presented the first ^{14}N MAS NMR spectrum of an amino acid, exemplified by the spectrum of L-alanine. However, apparently only the center part of the spectrum has been acquired (probably for experimental reasons), because the spectrum presented is characterized by only 15 ssbs for a spinning speed of 5.3 kHz and is approximately 80 kHz wide. For a ^{14}N quadrupolar coupling of 1.2 MHz, which is about the magnitude of C_Q determined by NQR for amino acids, the observation on the order of at least 200 ssbs is expected. This is about a factor 13 higher than seen in the spectrum by Khitrin and Fung [5]. In none of the studies of glycine [16] and L-alanine [5] has it been possible to determine the quadrupolar coupling constant (C_Q) and the associated asymmetry parameter (η_Q), most likely because of insufficient quality of the spectra.

In this paper we present the first observation of the complete manifold of ssbs in the ^{14}N MAS NMR spectra for several of the most common amino acids. We point out that all amino acids studied in this work exist in their zwitterionic form and therefore the ^{14}N MAS NMR spectra are those of a rotating $-NH_3^+$ group in the solid-state and not of an amino ($-NH_2$) group. The high quality of the spectra allows determination of precise values for C_Q and η_Q in these important biomolecules from computer simulation/fitting. Furthermore, since several amino acids crystallize with two molecules in the asymmetric unit, the two non-equivalent nitrogen sites for these molecules are clearly detected/distinguished in the ^{14}N MAS NMR spectra and two different sets of C_Q, η_Q values are determined from these spectra. In general terms, this work presents the first complete ^{14}N MAS NMR spectra of compounds characterized by C_Q as large as 1.2 MHz and a pioneering improvement in the quality of the spectra as compared to the ^{14}N MAS experiments on the nitrate ion [1,2] is achieved.

2. Experimental section

2.1. Materials

All compounds used in this work, i.e., glycine, L-alanine, L-cysteine, L-isoleucine, L-leucine, L-methionine, L-serine, L-valine, and $Pb(NO_3)_2$ are commercially available and were used without further purification. The sample of glycine was shown to be the α-polymorph by comparison of the experimentally determined value for the $T_1(^{13}C)$ relaxation time and the ^{13}C-$\{^1H\}$ cross-polarization time for the carboxylic carbon with values from the literature [17].

2.2. ^{14}N MAS and ^{15}N CP/MAS NMR spectroscopy

^{14}N MAS and ^{15}N cross-polarization (CP)/MAS NMR experiments were performed on a Varian *Unity* INOVA-600 spectrometer equipped with a 14.1 T wide-bore magnet and employing radio frequencies (rf) of 43.34 and 62.15 MHz, respectively. A Varian/Chemagnetics broadband low-γ frequency 7.5 mm T3 CP/MAS probe based on transmission line technology was used. The probe has a maximum spinning speed of 7 kHz, and its speed may be stabilized to <1 Hz for the 7.5 mm o.d. zirconia rotor using the Varian/Chemagnetics MAS speed controller and a highly pressure-stabilized air supply. The δ-scales for the ^{14}N and ^{15}N spectra are referenced to the narrow resonance (~0.3 ppm) of an external sample of NH_4Cl and $^{15}NH_4Cl$, respectively. The magic angle of $\theta = 54.736°$ ($3\cos^2\theta - 1 = 0$) was adjusted to the highest possible accuracy employing the ^{14}N MAS NMR spectrum of $Pb(NO_3)_2$, i.e., $\Delta\theta < \pm 0.005°$. However, upon sample (rotor) change, the angle may change slightly, up to $\pm 0.01°$, as has been noticed on several occasions by comparison with computer simulations of the spectra. All the other experimental set-ups were performed as reported elsewhere [1,2]. Acquisition of the ^{14}N MAS NMR spectra employed single-pulse excitation with $\tau_P = 1$ μs ($\tau_P^{90} = 6.3$ μs), a spinning speed of 6 kHz, a spectral width of 2 MHz, and a repetition delay of 2 s. ^1H decoupling during acquisition of the FIDs was not employed for two reasons: (i) the line width of the ssbs depends only marginally on the use of ^1H decoupling (less than a 25% reduction in line width is observed for the present experiments on the amino acids) but highly on the magic-angle setting; (ii) more importantly, the low-pass filter required in the observe channel for ^1H decoupling highly affects the rf bandwidth for the low-^{14}N frequency, independent of its design (Chebyshev, Bessel, etc.) and

quality. This results in an apparent high Q ($Q \sim 220$) for the observe channel (see Section 3). Although different types of low-pass filters have been constructed and tested, it is observed that the optimum performance/quality for the ^{14}N MAS spectra is achieved without a filter in the line of the observe channel. We are currently investigating an alternative filter design or other modifications which will allow ^{1}H decoupling to be performed without intensity suppression in the wings of wideband ^{14}N MAS NMR spectra.

The ^{15}N CP/MAS NMR spectra were recorded with the purpose of determining the isotropic ^{15}N chemical shifts for comparison with those obtained from the ^{14}N MAS NMR experiments and for obtaining an upper limit for the ^{15}N (^{14}N) chemical shift anisotropy (CSA). The ^{15}N CP/MAS NMR spectra used a contact time of 5 ms, a repetition delay of 4 s, and a spectral width of 100 kHz. Adjustment of the Hartmann–Hahn match was performed using a sample of $^{15}NH_4Cl$.

2.3. Simulations

All spectra were analyzed by computer simulation/iterative fitting on a Sun Microsystem Ultra 5 workstation using the STARS solid-state NMR software package developed in our laboratory [18–21] and incorporated into the Varian VNMR software. A few new features have been incorporated into the STARS software in order to fully appreciate the effects of many experimental factors, as already discussed in a recent investigation [2]. The quadrupolar coupling parameters employed in the simulations using STARS are related to the principal elements of the electric-field gradient tensor (V) by

$$C_Q = \frac{eQV_{zz}}{h}, \tag{1}$$

$$\eta_Q = \frac{V_{yy} - V_{xx}}{V_{zz}}, \tag{2}$$

where the principal tensor elements are defined by

$$V_{xx} + V_{yy} + V_{zz} = 0 \quad |V_{zz}| \geqslant |V_{xx}| \geqslant |V_{yy}|. \tag{3}$$

Because of the extremely small nitrogen CSA for the $-NH_3^+$ group in the amino acids as observed from their ^{15}N CP/MAS NMR spectra, i.e., $\delta_\sigma(^{15}N) = |\delta_{zz} - \delta_{iso}| < 10$ ppm (or the span of the chemical shift tensor $|\Omega| = |\delta_{zz} - \delta_{xx}| < 15$ ppm), the effect of the ^{14}N CSA on the appearance of the ^{14}N MAS NMR spectra can be neglected and is not considered in the simulations for the amino acids.

3. Results and discussion

Several experimental problems arise in the acquisition of the ^{14}N MAS NMR spectra and are attributable to the intrinsic characteristics of the ^{14}N nucleus, in particular its low-γ properties. The importance of a careful experimental set-up has already been discussed in a previous study [3]. Here we discuss some further experimental aspects which must be considered in recording ^{14}N MAS spectra of the amino acids, i.e., for ^{14}N quadrupole couplings $C_Q(^{14}N) \geqslant 1$ MHz. First, it is essential that a perfectly stable spinning speed, i.e., with a precision of ± 1 Hz, is maintained throughout the experiment. If this is not the case, the ssbs across the spectrum are broadened proportionally to their distance from the isotropic resonance. As a consequence, the simulation/fitting of the lineshape for the ssbs is not possible since the experimental lineshapes of the ssbs are distorted. Second, an even more serious issue appears to be the "apparent" high Q of the probe ($Q \sim 220$) combined with the low-NMR frequency of the ^{14}N nucleus ($\nu_0 = 43.34$ MHz at 14.1 T). This results in an extensive suppression of the outer regions of the ^{14}N MAS spectra, as already observed and discussed in our study of the nitrate ion [1]. High-Q probes are commonly employed in MAS NMR spectroscopy for sensitivity reasons, however, their use in ^{14}N MAS NMR appears to exert a severe impact on the appearance of spectra for $C_Q(^{14}N) > 0.3$ MHz. Thus, for the amino acids usually characterized by $C_Q(^{14}N) > 1$ MHz we predict the envelope of ssbs to appear highly distorted because of suppression of the ssb intensities into the noise level in the wings of the spectra. In practice this may hinder a complete analysis of the spectra in terms of the quadrupole coupling parameters C_Q and η_Q.

However, in the course of adjusting the magic angle employing ^{14}N MAS NMR of a sample of $Pb(NO_3)_2$ (vide supra), a ^{14}N MAS spectrum studied earlier in detail in our laboratory [1], it is observed that, contrary to the higher-frequency NMR nuclei, the appearance of the spectrum is extremely sensitive to the experimental set-up around the preamplifier and probe. Most importantly, for example removing the highly ideal low-pass filter (K&L Microwave), generally inserted between the preamplifier and the ^{14}N observe channel of the probe, eliminates the intensity suppression in the outer wings of the spectrum. The resulting spectrum now appears as if a dramatic change has occurred in the "apparent" Q of the probe. We should note that the program STARS includes a feature that can easily compensate for the effect of the probe Q in the simulation of the spectra. The above-mentioned effects are illustrated in Fig. 1, where two quite different experimental spectra for the same sample of $Pb(NO_3)_2$ are presented. The spectrum in Fig. 1A is acquired with the usual experimental set-up, i.e., including the low-pass filter in-line as in our earlier studies of nitrate ions [1,2]. The spectrum is characterized by an increasing suppression of the ssbs with respect to their distance from the carrier frequency. This trend can be simulated simply by adopting a rf bandwidth of 0.2 MHz

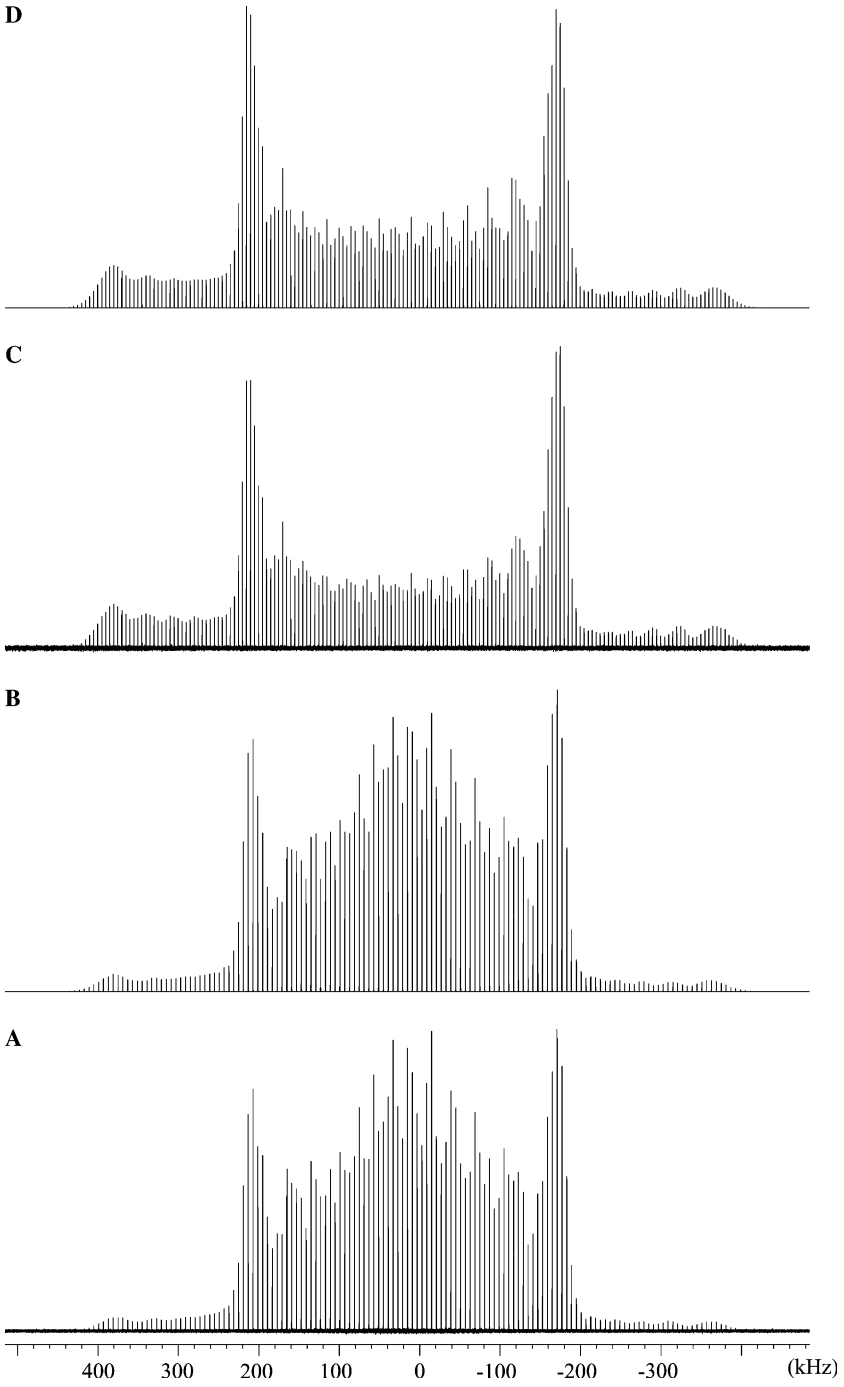

Fig. 1. Experimental and simulated ^{14}N MAS NMR spectra (43.34 MHz at 14.1 T) of $Pb(NO_3)_2$ for $\nu_r = 6000$ Hz. The experimental spectra in (A), 18,000 scans, and (C), 16,000 scans, illustrate the effect of acquiring the experimental spectra with and without a K&L low-pass filter in the line between the probe and the preamplifier, respectively (see text). The simulated spectrum in (B) results from least-squares optimization to the experimental spectrum in (A) using the NMR parameters in Table 1, a rf bandwidth of 0.2 MHz, and a deviation $\Delta\theta = -0.002°$ from exact setting of the magic angle. The simulated spectrum in (D) results from least-squares optimization to the experimental spectrum in (C) using the NMR parameters in Table 1, a rf bandwidth of 0.9 MHz, and a deviation $\Delta\theta = -0.005°$ from exact setting of the magic angle.

corresponding to $\nu_0/Q = 43.34\,\text{MHz}/220 = 0.2\,\text{MHz}$ and using the NMR parameters determined earlier [1], as illustrated in the simulated spectrum of Fig. 1B. A ^{14}N MAS NMR spectrum acquired following removal of the in-line low-pass filter is shown in Fig. 1C. This spectrum illustrates that the suppression of the outer parts of the spectrum, as observed in Fig. 1A, has been completely eliminated. A convincing simulation of the experimental spectrum (Fig. 1C) is shown in Fig. 1D and is achieved directly by adopting the same parameters as used for the

simulation in Fig. 1B, however, changing the value of the rf bandwidth from 0.2 MHz to ~0.9 MHz ($Q \sim 50$). Although the Q value of the probe at 43.34 MHz (^{14}N) is independently measured to be $Q \sim 130$, the reason for the change of the "apparent" Q from $Q \sim 220$ to $Q \sim 50$, induced by removing the in-line low-pass filter between the probe and preamp, is presently being investigated.

The effect of the low-pass filter shown in Fig. 1 for $Pb(NO_3)_2$ appears to be even more dramatic on the ^{14}N MAS spectra for the amino acids. This is illustrated by the ^{14}N MAS spectra of L-alanine obtained with (Fig. 2A) and without (Fig. 2B) the low-pass filter inserted in the transmit/receive coax cable between the preamplifier and the probe. As seen, the L-alanine spectrum in Fig. 2A suffers extreme intensity suppression in the regions away from the center of the spectrum, thereby hiding both discontinuities and edges of the spectrum in the noise level. Thus, determination of precise values for the quadrupole coupling parameters would be very difficult from the spectrum in Fig. 2A. On the contrary, the ^{14}N MAS spectrum of L-alanine recorded without the low-pass filter shows up with well-defined discontinuities and edges (Fig. 2B). Iterative fitting of simulated spectra to the experimental spectrum in Fig. 2B leads to the quadrupole coupling parameters for L-alanine listed in Table 1 where the results for all the amino acids investigated in this work are summa-

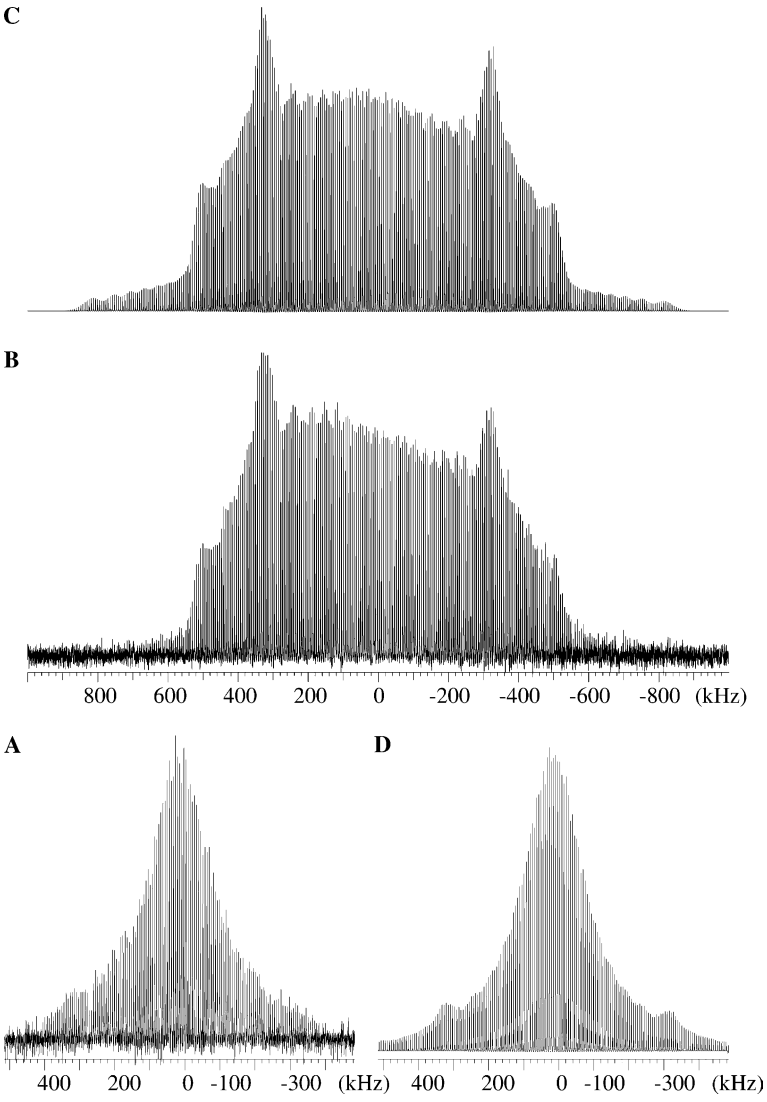

Fig. 2. Experimental and simulated ^{14}N MAS NMR spectra (43.34 MHz at 14.1 T) of L-alanine for $\nu_r = 6000$ Hz. The experimental spectra in (A), 18,000 scans, and (B), 120,000 scans, illustrate the effect of acquiring the spectra with and without a K&L low-pass filter in the line between the probe and the preamplifier, respectively (see text). The simulated spectrum in (C) results from least-squares optimization to the experimental spectrum in (B) using the NMR parameters in Table 1, a rf bandwidth equal to 2 MHz, and a rf offset of 93 kHz. The simulated spectrum in (D) uses exactly the same parameters as for the spectrum in (C), except that the rf bandwidth is equal to 0.2 MHz, corresponding to an apparent high-Q of approximately 220 for the probe.

Table 1
^{14}N Quadrupole coupling parameters (C_Q, η_Q) and isotropic chemical shifts (δ_{iso}) from ^{14}N and ^{15}N MAS NMR of some amino acids[a]

Amino acid		C_Q (MHz)	η_Q	δ_{iso} (^{14}N) (ppm)	δ_{iso} (^{15}N) (ppm)
Glycine		1.17	0.51	−6.3	−6.4
		1.182 [13]	0.54 [13]		
		1.249 [10]	0.501 [10]		
		1.247 [11]	0.502 [11]		
L-Alanine		1.14	0.24	3.1	2.8
		1.205 [11]	0.261 [11]		
L-Serine		1.17	0.17	−2.2	−4.0
		1.167 [11]	0.361 [11]		
L-Cysteine[b]		1.22	0.50	−0.3	−0.3
	(1)	1.273 [11]	0.64 [11]		
	(2)	1.195 [11]	0.13 [11]		
L-Valine	(1)	1.17	0.17	1.8	2.1
	(2)	1.19	0.25	2.1	
L-Leucine	(1)	1.13	0.08	5.5	4.1
	(2)	1.19	0.33	3.0	
L-Isoleucine	(1)	1.16	0.29	1.3	1.3
	(2)	1.20	0.11	1.5	
L-Methionine	(1)	1.16	0.17	5.5	4.8
	(2)	1.22	0.37	5.1	

[a] The error limits for C_Q, η_Q, δ_{iso} (^{14}N), and δ_{iso} (^{15}N) are ±0.03 MHz, ±0.03, ±1 ppm, and ±0.3 ppm, respectively. Where possible the parameters are compared with values determined earlier from ^{14}N NQR and ^{14}N SC NMR (indicated with references to the literature). For amino acids with two molecules in the asymmetric unit, two sets of parameters are determined and marked as (1) and (2).

[b] L-Cysteine can crystallize in two different space groups, i.e., either orthorhombic or monoclinic (see text).

rized. The simulated spectrum for L-alanine using these parameters (Fig. 2C) is in good agreement with the experimental spectrum. We note that the parameters employed for the simulation in Fig. 2C also reproduces the experimental spectrum characterized by the "apparent" high probe Q in Fig. 2A, as illustrated by the simulation in Fig. 2D, where only the rf bandwidth has been changed from 0.9 to 0.2 MHz (i.e., to an "apparent" $Q \sim 220$).

As it may have already been noticed, the manifold of ssbs in the experimental spectrum of Fig. 2B suffers a "tilt" in the intensities of the ssbs with respect to the center of the spectrum. A similar "tilt" is often observed for the two "horns" in static solid-state ^{2}H NMR spectra. This "tilt" is related to a non-optimal length of either the lambda-quarter ($\lambda/4$) cable in the preamplifier or of the cable between the preamplifier and the probe. Changing the length of either of these cables causes a change in the "tilt" of the spectrum. These changes are equivalent to a minor shift in the excitation/detection profile for the probe and corresponds to a rf offset/phase shift relative to ideal rf excitation at the center of the spectrum. This distortion is easily handled by the STARS simulation/fitting software program through variation of the rf offset relative to the isotropic shift. However, an optimum experimental set-up of the cable lengths (within a few centimeters) is possible. The effect of such an optimization is illustrated in Fig. 3A, which shows an experimental spectrum of L-alanine where the tilting of the two "horns" and the two outer edges has been almost completely eliminated by adopting proper cable lengths. However, optimization of cable lengths is not the only factor capable of introducing a "tilt" in the experimental spectrum. An additional factor appears to be slight deviations in adjustment of the rotor axis from the exact setting of the magic angle as justified by the experimental and simulated spectra of L-alanine in Fig. 3. As illustrated by the spectrum of L-alanine (Fig. 3A), a correct choice of cable lengths as well as a careful and precise adjustment of the magic angle produces a spectrum with minimum "tilt," where the two discontinuities and the outer shoulders are characterized by almost equal heights. The result of the simulation illustrated in Fig. 3B (employing a rf offset of only 30 kHz) confirms that the rotor axis coincides with the magic angle. Imposing an offset on the rotor axis of $\Delta\theta = -0.02°$, the simulation in Fig. 3C shows that the predominant discontinuities in the spectrum exhibit different heights and that the overall shape of the manifold of ssbs is "tilted." We note that while a small negative offset ($\Delta\theta$) from the magic angle causes a "tilt" in one direction, an offset of the same magnitude, but opposite sign causes a reversal in the "tilt" of the spectrum, as seen from a comparison of the simulations in Figs. 3B–D. Thus, we conclude that the experimental ^{14}N MAS NMR spectra of highest quality for the amino acids are obtained without the use of a low-pass filter and following proper adjustments of cable lengths and the rotor angle using a sample of $Pb(NO_3)_2$.

For the sample of L-alanine, the spectrum of highest and mostly ideal quality is that illustrated in Fig. 3A. Here, the manifold of ssbs is dominated by clear and well-resolved edges in the outer part of the spectrum and by two singularities of nearly equal height, which are

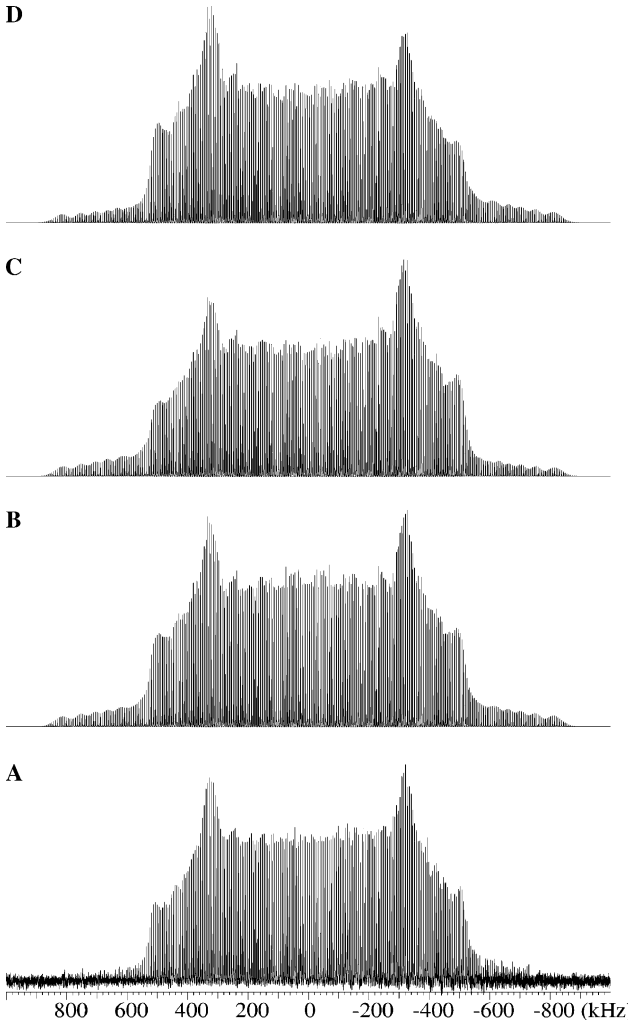

Fig. 3. Experimental and simulated ^{14}N MAS NMR spectra of L-alanine for $\nu_r = 6000$ Hz. The experimental spectrum in (A), 120,000 scans, is acquired using an optimized length for the cable between the probe and preamplifier (slightly shorter compared to the cable used for the spectrum in Fig. 2B) (see text). The simulated spectra in (B–D) use the quadrupolar coupling parameters shown in Table 1, a rf bandwidth equal to 2 MHz, a rf offset of −30 kHz, and the following deviations $\Delta\theta$ from exact setting of the magic angle: (B) $\Delta\theta = 0°$, (C) $\Delta\theta = -0.02°$, and (D) $\Delta\theta = +0.02°$ (see text).

situated near the edges. The appearance of this spectrum differs from that illustrated in Fig. 2B, where the singularities are characterized by different heights and the overall spectrum is somewhat tilted. It is important to note that both experimental spectra (Figs. 2B and 3A) can be simulated using STARS, employing the same set of quadrupole coupling parameters (see Table 1) as illustrated by the simulations in Figs. 2C and 3B. This implies that even a non-optimal set-up of the experiment would allow extraction of the correct set of parameters from the spectrum recorded. The differences in the appearance of the two simulations in Figs. 2C and 3B are induced by differences in the values used for the rf offset (93 and −30 kHz, respectively), a consequence of the different lengths used for the $\lambda/4$ cable on the preamplifier. The parameters determined from the ^{14}N MAS NMR spectra are in good agreement with those reported earlier from a ^{14}N NQR study by Edmonds [10]. The slight differences observed for the quadrupole coupling parameters determined from the two different techniques (C_Q, $\eta_Q = 1.145$ MHz, 0.241 and 1.205 MHz, 0.261, respectively) can be justified by the difference in temperature at which the two investigations have been performed, ambient temperature (^{14}N MAS NMR) and 77 K (^{14}N NQR).

The ^{14}N MAS NMR spectrum of L-serine shown in Fig. 4A is characterized by well-defined singularities and edges quite similar to the envelope of ssbs observed for the spectrum of L-alanine. The main difference between the experimental spectra of these two amino acids is observed to be a more pronounced tilt present for the spectrum of L-serine, a distortion that was hardly noticeable for the spectrum of L-alanine in Fig. 3A. Since both spectra have been acquired with exactly the same experimental set-up, the most plausible reason for the difference in their appearance would be a slight deviation $\Delta\theta$ of the rotor axis from the exact magic angle. This is confirmed by the optimized computer simulation in Fig. 4B which employed $\Delta\theta = -0.004$. The overall resemblance of the manifolds of ssbs in the spectra for L-serine and L-alanine points towards quite similar values for the quadrupolar coupling parameters of the two compounds, which is confirmed by the results of the iterative fitting (see Table 1). The quadrupolar coupling parameters determined for L-serine ($C_Q = 1.167$ MHz and $\eta_Q = 0.17$) are in good agreement with the data determined from a ^{14}N NQR study by Edmonds [10]

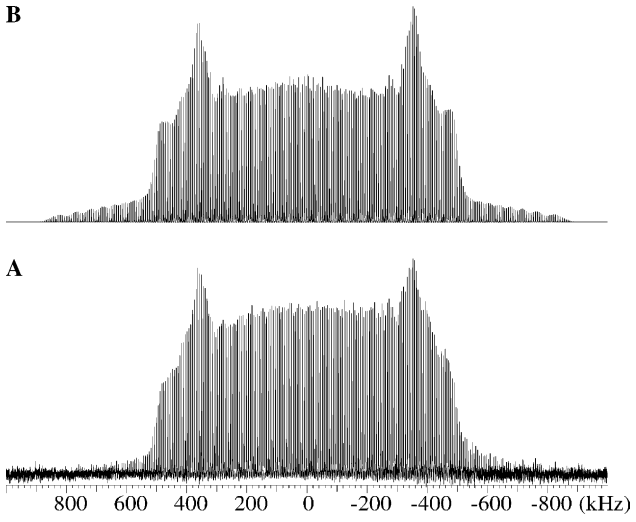

Fig. 4. Experimental (A) and simulated (B) ^{14}N MAS NMR spectra of L-serine for $\nu_r = 6000$ Hz. The spectrum in (A), 115,000 scans, is acquired using the same experimental conditions as for the spectrum in Fig. 3. The simulated spectrum uses the parameters shown in Table 1, a rf bandwidth equal to 2 MHz, a rf offset of −30 kHz, and a deviation $\Delta\theta$ from the magic angle of $\Delta\theta = -0.004°$.

($C_Q = 1.215$ MHz and $\eta_Q = 0.361$) considering the low temperature (77 K) used in that study.

The ^{14}N MAS NMR spectrum of glycine (Fig. 5A) shows clear deviations from those of both L-alanine and L-serine. First, the positions of the two singularities are closer to the center of the spectrum, which indicates a somewhat larger value for the asymmetry parameter η_Q as compared to the values for L-alanine and L-serine. Second, the spectrum of glycine in Fig. 5A displays a nearly linear slope for the decrease of the intensities for the outer ssbs, a slope which partially hides the position of the outer edges of the spectrum in the noise level. The quadrupole coupling parameters ($C_Q = 1.173$ MHz and $\eta_Q = 0.52$) determined from optimized fitting of simulated to experimental spectra correspond to the simulated spectrum shown in Fig. 5B for glycine which is in excellent agreement with the experimental spectrum. These optimized C_Q, η_Q parameters (Table 1) are in accord with the values determined by Haberkorn et al. [12] from a ^{14}N single-crystal study at ambient temperature ($C_Q = 1.182$ MHz and $\eta_Q = 0.54$). Values determined from ^{14}N NQR at 77 and 90 K by Edmonds [10] (C_Q, $\eta_Q = 1.249$ MHz, 0.501 and C_Q, $\eta_Q = 1.247$ MHz, 0.502, respectively) differ only slightly from the ambient temperature data determined here and by Haberkorn et al. [12].

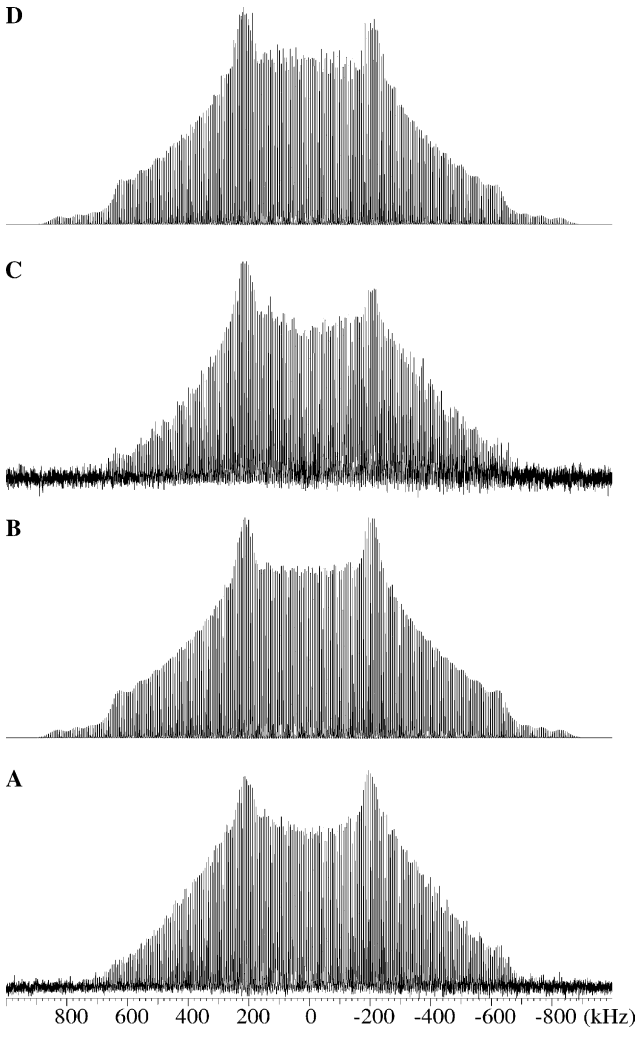

Fig. 5. ^{14}N MAS NMR spectra of α-glycine and L-cysteine acquired for $\nu_r = 6000$ Hz. (A) Experimental (80,000 scans) and (B) simulated ^{14}N MAS NMR spectrum of α-glycine. (C) Experimental (123,000 scans) and (D) simulated ^{14}N MAS NMR spectrum of L-cysteine. The two simulated spectra are obtained using the quadrupolar coupling parameters shown in Table 1, a rf bandwidth equal to 2 MHz, a rf offset of −30 kHz, and exact setting of the magic angle ($\Delta\theta = 0.000°$).

L-Cysteine crystallizes into two different polymorphs, orthorhombic [22,23] and monoclinic [24,25], which are characterized by the presence of one and two molecules of L-cysteine in the asymmetric unit, respectively. In a low-temperature ^{14}N NQR study Edmonds et al. [9] extracted two set of quadrupole coupling parameters characterized by quite similar quadrupolar coupling constants but different asymmetry parameters (see Table 1). It is noteworthy that the data determined at 77 K for one set of parameters ($C_Q = 1.273$ MHz and $\eta_Q = 0.64$) are quite similar to those determined for glycine ($C_Q = 1.249$ MHz and $\eta_Q = 0.501$). Because of the detection of two sets of quadrupole coupling parameters, the crystal structure of their sample was assigned the monoclinic form with reference to the crystal structure reported by Harding and Long [24]. The ^{14}N MAS NMR spectrum of the L-cysteine sample studied in the present work is illustrated in Fig. 5C. This spectrum exhibits an envelope of ssbs similar to that for glycine and similarly the spectrum can be simulated as shown in Fig. 5D using only one set of optimized quadrupole coupling parameters (see Table 1). If two molecules with quite different asymmetry parameters and similar magnitudes for C_Q would have been present in the asymmetric unit of the crystal structure for our L-cysteine sample, this would clearly have been observed in the ^{14}N MAS NMR spectra (vide infra). Thus, on the basis of the ^{14}N MAS NMR spectrum we assign the crystal structure of the L-cysteine sample used in this study to be that of the orthorhombic polymorph [22,23]. This has been confirmed by a single-crystal XRD study which shows that the polycrystalline sample of L-cysteine studied here has the orthorhombic crystal structure with only one molecule in the asymmetric unit.

Contrary to the spectrum of the L-cysteine sample, the ^{14}N MAS spectra of L-leucine, L-isoleucine, L-valine, and L-methionine reported in Figs. 6A and C and 7A and C, respectively, illustrate the effect of the presence of two molecules in the asymmetric unit. These spectra clearly show the presence of two pairs of well-defined singularities along with the corresponding sets of edges in the outer wings of the spectra. Since the linewidth of the ssbs are on the order of several hundred Hz (about 8–10 ppm) the small chemical shift difference between the two molecules in the asymmetric unit does not allow the two overlapping spectra to be resolved for

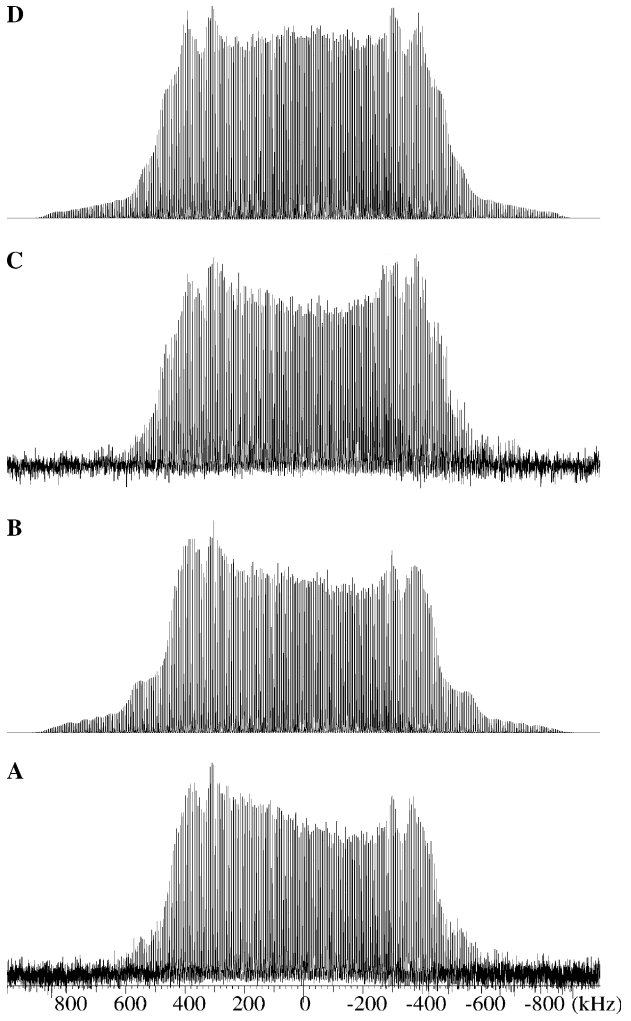

Fig. 6. ^{14}N MAS NMR spectra L-leucine and L-isoleucine acquired for $\nu_r = 6000$ Hz. (A) Experimental (130,000 scans) and (B) simulated ^{14}N MAS NMR spectrum of L-leucine. (C) Experimental (114,000 scans) and (D) simulated ^{14}N MAS NMR spectrum of L-isoleucine. The two simulated spectra are obtained using the parameters shown in Table 1, a rf bandwidth equal to 2 MHz, a rf offset of −30 kHz, and deviations from the exact magic-angle setting of (B) $\Delta\theta = -0.004°$, and (D) $\Delta\theta = 0.001°$.

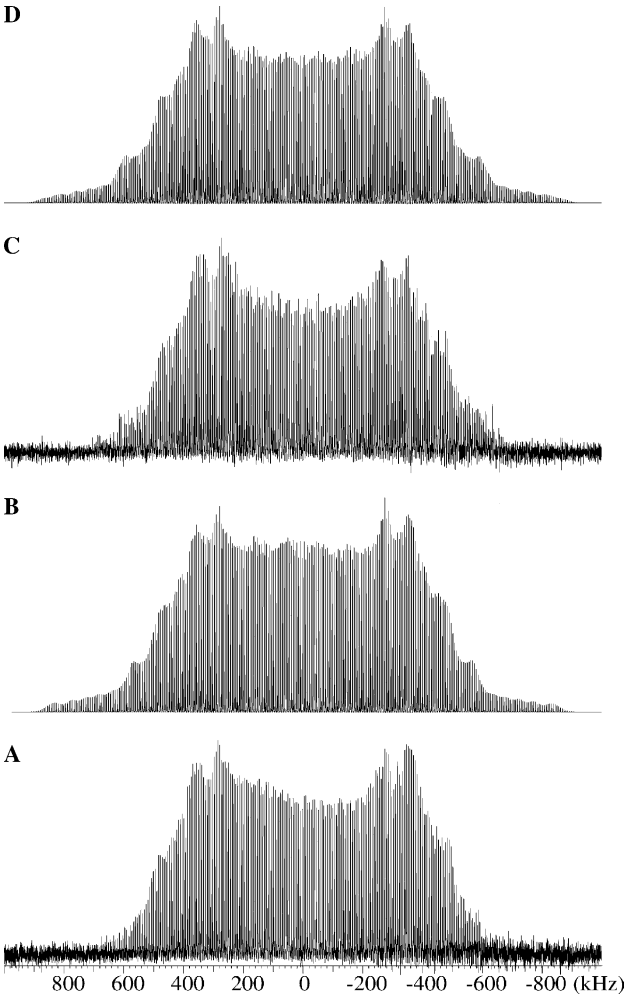

Fig. 7. ^{14}N MAS NMR spectra of L-valine and L-methionine acquired for $\nu_r = 6000$ Hz. (A) Experimental (160,000 scans) and (D) simulated ^{14}N MAS NMR spectrum of L-valine. (C) Experimental (170,000 scans) and (B) simulated ^{14}N MAS NMR spectrum of L-methionine. The two simulated spectra are obtained using the quadrupolar coupling parameters shown in Table 1, a rf bandwidth equal to 2 MHz, a rf offset of −30 kHz, and deviations from the exact magic-angle setting of (B) $\Delta\theta = -0.010°$ and (D) $\Delta\theta = 0.000°$.

any of these four amino acids. Thus, the ssbs for the two molecules in the asymmetric units overlap throughout the complete spectra and the analysis requires the assumption of the presence of two non-equivalent sites and a correct combination of the pairs of singularities with their corresponding inner or outer edges. From trial and error simulations it is shown that fitting of the simulated to experimental spectra is only possible when the pair of inner singularities are linked to the outer edges and vice versa for the outer singularities. The results from the analysis of the experimental spectra of L-leucine (Fig. 6A), L-isoleucine (Fig. 6C), L-valine (Fig. 7A), and L-methionine (Fig. 7C) using the STARS software are summarized in Table 1 for each of the two non-equivalent ^{14}N nuclei in these amino acids. It is noted that the ^{14}N isotropic shifts (δ_{iso} (^{14}N)) obtained for the two non-equivalent ^{14}N nuclei are in good agreement with the δ_{iso} (^{15}N) values (Table 1) determined from the ^{1}H decoupled ^{15}N CP/MAS spectra which, however, cannot be resolved into two separate resonances. The corresponding simulated ^{14}N MAS spectra using the two sets of quadrupolar coupling parameters for each compound are shown above the experimental spectra in Figs. 6 and 7. To our knowledge no data for the quadrupolar coupling parameters have previously been reported for these four amino acids. The ^{14}N NQR spectrum of L-methionine has been reported by Blinc et al. [8], but unfortunately a final assignment of the observed lines with subsequent determination of the quadrupolar coupling parameters was not possible.

The ^{14}N quadrupole coupling data determined in this work (Table 1) show that the amino acids exhibit very similar quadrupole couplings (i.e., $1.13\,\text{MHz} \leqslant C_Q \leqslant 1.22\,\text{MHz}$) whereas some variation is observed for the corresponding asymmetry parameters. These C_Q values are quite similar to those determined for the -NH_3^+ group in some monoalkyl ammonium (R-NH_3^+) samples ($1.0 \leqslant C_Q \leqslant 1.2\,\text{MHz}$) from ^{14}N MAS NMR in our laboratory (unpublished data). Assignments of the two sets of ^{14}N quadrupole coupling parameters, observed for L-leucine, L-isoleucine, L-valine, and L-methionine, to the specific molecules in the asymmetric units of their crystal structures are hardly possible on basis of simple methods for modeling the electronic structure around the nitrogen atoms. This is primarily due to the fact that the structural refinements of the X-ray diffraction data reported for these amino acids do not include the hydrogen atoms [26–28] or assume normalized N–H and C–H bond distances [29]. Moreover, from the reported structures it is apparent that hydrogen bonding has an important impact on the specific conformation of the individual amino acid molecules in the crystal structures. For example, from the crystal structures recently redetermined for L-valine and L-methionine, the conformational differences observed for the two molecules A and B in their asymmetric units [29] (and induced by the hydrogen bonding networks) must be related to the difference in asymmetry parameters (η_Q) for the -NH_3^+ groups in A and B. However, assignment of the η_Q values to the individual molecules A and B may require density functional theory (DFT) calculations [30] or similar advanced approaches considering the role of the N–H$\cdots$O hydrogen bonds in these crystal structures, in order to elucidate the relationship between these conformations and the ^{14}N asymmetry parameters.

The C_Q values determined in this study for the –NH_3^+ group in amino acids represent an increase of about a factor 2 in magnitude for the ^{14}N quadrupolar coupling constants that has so far been determined from complete ^{14}N MAS NMR spectra (e.g., for the nitrate ions $C_Q \sim 0.5$–0.7 MHz) [1]. An additional increasing jump by a factor of 2 in C_Q, accompanied by further improvements in the experimental technology of ^{14}N MAS NMR should allow characterization of –NH_2 or amide groups in basic amino acids or peptides, where $C_Q \sim 2$–3 MHz. Simulations show that the experimental challenges in such studies require coping with low-intensity ^{14}N MAS ssbs caused by severe second-order linebroadening and extending over a spectral width of 5 MHz.

4. Conclusions

Following optimization of experimental conditions, solid-state ^{14}N MAS NMR spectroscopy is shown to be a valuable tool for characterization and studies of amino acids. Thus, the complete ^{14}N MAS NMR spectra, covering a spectral width in excess of 1 MHz, are presented for several amino acids for the first time. Computer simulations combined with fitting of simulated to experimental ssb intensities result in the determination of precise values for the ^{14}N quadrupole coupling constants and asymmetry parameters for the nitrogen sites in the solid phase of these molecules. For some of the amino acids the ^{14}N MAS NMR spectra exhibit overlap between the spectra representing two different nitrogen sites in accordance with their crystal structures, which show the presence of two non-equivalent amino acids in the asymmetric unit. Computer analysis of these spectra results in two different sets of quadrupole coupling parameters. Assignments of the two pairs of C_Q and η_Q values to the two distinct molecules in the asymmetric unit are not possible at this time and may require advanced theoretical calculations. Some of the quadrupole coupling parameters determined in this study may be compared to values reported earlier using ^{14}N nuclear quadrupole resonance (NQR) or single-crystal ^{14}N NMR spectroscopy. Excellent agreements between the presently determined parameters and the earlier reported data are observed.

Acknowledgments

We are grateful to Dr. Rita G. Hazell of this department for confirming the orthorhombic crystal structure for our sample of L-cysteine by single-crystal XRD. The use of the facilities at the Instrument Centre for Solid-State NMR Spectroscopy, University of Aarhus, sponsored by Danish Natural Research Council, the Danish Technical Science Research Counsil, Teknologistyrelsen, Carlsbergfondet, and Direktør Ib Henriksens Fond, is acknowledged. Financial support from the two Danish Research Councils (J.nr. 2020-00-0018 and J.nr. 0001237) is acknowledged.

References

[1] H.J. Jakobsen, H. Bildsøe, J. Skibsted, T. Giavani, ^{14}N MAS NMR spectroscopy: the nitrate ion, J. Am. Chem. Soc. 123 (2001) 5098–5099.

[2] T. Giavani, H. Bildsøe, J. Skibsted, H.J. Jakobsen, ^{14}N MAS NMR spectroscopy and quadrupole coupling data in characterization of the IV⇒III phase transition in ammonium nitrate, J. Phys. Chem. B. 106 (2002) 3026–3032.

[3] T. Giavani, K. Johannsen, C.J. Jacobsen, N. Blom, H. Bildsøe, J. Skibsted, H.J. Jakobsen, Unusual observation of nitrogen chemical shift anisotropies in tetraalkylammonium halides by ^{14}N MAS NMR spectroscopy, Solid State Nucl. Magn. Reson. 24 (2003) 218–235.

[4] K. Ermolaev, B.M. Fung, High-resolution ^{14}N NMR in polycrystalline solids, J. Chem. Phys. 110 (1999) 7977–7982.

[5] A.K. Khitrin, B.M. Fung, ^{14}N nuclear magnetic resonance of polycrystalline solids with fast spinning at or very near the magic angle, J. Chem. Phys. 111 (1999) 8963–8969.
[6] D.T. Edmonds, P.A. Speight, Nitrogen quadrupole resonance in amino acids, Phys. Lett. 34A (1971) 325–326.
[7] D.T. Edmonds, P.A. Speight, Nuclear quadrupole resonance of ^{14}N in pyrimidines, purines and their nucleosides, J. Magn. Reson. 6 (1972) 265–273.
[8] R. Blinc, M. Mali, R. Osredkar, A. Prelesnik, J. Seliger, I. Zupancic, L. Ehrenberg, ^{14}N NQR spectroscopy of some amino acids and nucleic bases via double resonance in the laboratory frame, J. Chem. Phys. 57 (1972) 5087–5093.
[9] D.T. Edmonds, C.P. Summers, ^{14}N pure quadrupole resonance in solid amino acids, J. Magn. Reson. 12 (1973) 134–142.
[10] D.T. Edmonds, Nuclear quadrupole double resonance, Phys. Rep. 29 (1977) 233–290.
[11] L.-O. Andersson, M. Gourdji, L. Guibé, W.G. Proctor, Détermination, par résonance magnétique nucléare, du couplage quadripolaire de l'azote du glycocolle, C. R. Acad. Sci. Paris 267B (1968) 803–805.
[12] R.A. Haberkorn, R.E. Stark, H. van Willigen, R.G. Griffin, Determination of bond distances and bond angles by solid-state nuclear magnetic resonance. ^{13}C and ^{14}N NMR study of glycine, J. Am. Chem. Soc. 103 (1981) 2534–2539.
[13] C.A. McDowell, A. Naito, D.L. Sastry, K. Takegoshi, Determination of the ^{14}N quadrupole coupling tensors in a single crystal of *l*-histidine hydrochloride monohydrate by NMR spectroscopy, J. Magn. Reson. 69 (1986) 283–292.
[14] A. Naito, C.A. McDowell, Determination of the ^{14}N quadrupole coupling tensors and the ^{13}C chemical shielding tensors in a single crystal of L-asparagine monohydrate, J. Chem. Phys. 81 (1984) 4795–4803.
[15] A. Naito, S. Ganapathy, P. Raghunathan, C.A. McDowell, Determination of the ^{14}N quadrupole coupling tensor and the ^{13}C chemical shielding tensors in a single crystal of L-serine monohydrate, J. Chem. Phys. 79 (1983) 4173–4182.
[16] G. Jeschke, M. Jansen, High-resolution ^{14}N solid-state NMR spectroscopy, Angew. Chem. Int. Ed. 37 (1998) 1282–1283.
[17] M.J. Potrzebowski, P. Tekely, Y. Dusausoy, Comment to ^{13}C-NMR studies of α and γ polymorphs of glycine, Solid State Nucl. Magn. Reson. 11 (1998) 253–257.
[18] H.J. Jakobsen, J. Skibsted, H. Bildsøe, N.C. Nielsen, Magic-angle spinning NMR spectra of satellite transitions for quadrupolar nuclei in solids, J. Magn. Reson. 85 (1989) 173–180.
[19] J. Skibsted, N.C. Nielsen, H. Bildsøe, H.J. Jakobsen, Satellite transitions in MAS NMR spectra of quadrupolar nuclei, J. Magn. Reson. 95 (1991) 88–117.
[20] J. Skibsted, N.C. Nielsen, H. Bildsøe, H.J. Jakobsen, ^{51}V MAS NMR spectroscopy: determination of quadrupole and anisotropic shielding tensors, including the relative orientation of their principal-axis systems, Chem. Phys. Lett. 188 (1992) 405–412.
[21] J. Skibsted, N.C. Nielsen, H. Bildsøe, H.J. Jakobsen, Magnitudes and relative orientation of ^{51}V quadrupole coupling and anisotropic shielding tensors in metavanadates and KV_3O_8 from ^{51}V MAS NMR spectra. ^{23}Na quadrupole coupling parameters for α- and β-$NaVO_3$, J. Am. Chem. Soc. 115 (1993) 7351–7362.
[22] K.A. Kerr, J.P. Ashmore, Structure and conformation of orthorhombic L-cysteine, Acta Crystallogr. B 29 (1973) 2124–2127.
[23] K.A. Kerr, J.P. Ashmore, T. Koetzle, A neutron diffraction study of L-cysteine, Acta Crystallogr. B 31 (1975) 2022–2026.
[24] M.M. Harding, H.A. Long, The crystal and molecular structure of L-cysteine, Acta Crystallogr. B 24 (1968) 1096–1102.
[25] C.H. Görbitz, B. Dalhus, L-cysteine, monoclinic form, redetermination at 120 K, Acta Crystallogr. C 52 (1996) 1756–1759.
[26] M.M. Harding, R.M. Howieson, L-leucine, Acta Crystallogr. B 32 (1976) 633–634.
[27] K. Torii, Y. Iitaka, The crystal structure of L-isoleucine, Acta Crystallogr. B 27 (1971) 2237–2246.
[28] K. Torii, Y. Iitaka, The crystal structure of L-valine, Acta Crystallogr. B 26 (1970) 1317–1326.
[29] B. Dalhus, C.H. Görbitz, Crystal structures of hydrophobic amino acids I. Redeterminations of L-methionine and L-valine at 120 K, Acta Chem. Scand. 50 (1996) 544–548.
[30] V. Barone, C. Adamo, Proton transfer in the ground and lowest excited states of malonaldehyde: a comparative density functional and post-Hatree–Fock study, J. Chem. Phys. 105 (1996) 11007–11019.